



Open Access Articles

Delayed Survey of the 2011 Tohoku Tsunami in the Former Exclusion Zone in Minami-Soma, Fukushima Prefecture

The Faculty of Oregon State University has made this article openly available.
Please share how this access benefits you. Your story matters.

Citation	Sato, S., Okayasu, A., Yeh, H., Fritz, H. M., Tajima, Y., & Shimozone, T. (2014). Delayed survey of the 2011 Tohoku Tsunami in the former exclusion zone in Minami-Soma, Fukushima Prefecture. Pure and Applied Geophysics, 171(12), 3229-3240. doi:10.1007/s00024-014-0809-8
DOI	10.1007/s00024-014-0809-8
Publisher	Springer
Version	Accepted Manuscript
Terms of Use	http://cdss.library.oregonstate.edu/sa-termsofuse

Delayed survey of the 2011 Tohoku Tsunami in the former exclusion zone in Minami-Soma, Fukushima Prefecture

Shinji Sato¹⁾, Akio Okayasu²⁾, Harry Yeh³⁾, Hermann M. Fritz⁴⁾, Yoshimitsu Tajima¹⁾ and Takenori Shimozone¹⁾

- 1) Department of Civil Engineering, The University of Tokyo, 7-3-1 Hongo, Bunkyo-ku, Tokyo, JAPAN, email:sato@coastal.t.u-tokyo.ac.jp
- 2) Department of Ocean Sciences, Tokyo University of Marine Science and Technology, 4-5-7 Konan, Minato-ku, Tokyo, JAPAN
- 3) School of Civil and Construction Engineering, Oregon State University, Corvallis, OR 97331-3212, USA
- 4) School of Civil and Environmental Engineering, Georgia Institute of Technology, Atlanta, GA 30322, USA.

Abbreviated title: Tohoku Tsunami survey in Minami-Soma, Fukushima

Keywords: Tohoku Tsunami, inland tsunami heights, tsunami disaster followed by a nuclear accident, seawall performance

ABSTRACT

Post tsunami field surveys in the Minami-Soma exclusion zone in the Fukushima Prefecture were delayed for 15 months after the 2011 Tohoku tsunami. The area was subject to access restrictions until June 2012 due to high radiation levels caused by the meltdown at the Fukushima Dai-ichi Nuclear Power Plant. The distribution of the measured tsunami heights is presented in combination with observed infrastructure damage. The enhanced tsunami heights in the areas along the shoreline are attributed to wave reflection, funneling and splash-up at cliffs and seawalls, as well as the increased flow resistance as the tsunami plows through coastal pine-tree forests. Consequently, large tsunami heights exceeding 10 m were limited to areas within 500 m from the shoreline. Onshore profiles of the maximum inundation levels were dependent on inland

topography: tsunami heights increased inland in steep V-shaped valleys, while decaying with inundation distance along flat coastal plains. Tsunami flood levels in the coastal plains are affected by the extent of seawall damage: coastal flood levels are higher behind completely destroyed seawalls than behind partially damaged coastal defenses. Remnant seawalls provided valuable lessons to be implemented in future designs of tenacious structures based on the Japanese concept of ‘nebari’ representing resiliency to endure tsunami overflow as the original design height is exceeded.

1. Introduction

At 14:46 on March 11, 2011 (JST), a magnitude 9.0 earthquake struck the northeast coast of Japan, resulting from thrust faulting along the subduction zone between the Pacific and the North American Plates (Simons et al., 2011; Fujii et al., 2011). This earthquake generated catastrophic tsunamis, which severely impacted the Japanese Pacific coast. According to the Tohoku Earthquake Tsunami Joint Survey Group (TTSG, 2011), the measured maximum tsunami run-up heights reached nearly 40 m. This tsunami represents the largest tsunami event possibly within the last one thousand years in Japan. Significant casualties (15,884 fatalities with an additional missing 2,640 presumed dead as of January 10, 2014 according to National Police Agency) and tremendous damage to coastal cities and infrastructure were caused by this tsunami event, while the earthquake accounts for less than 1% of the fatalities. The tsunami inundation at the Fukushima Dai-ichi Nuclear Power Plant (NPP) resulted in the worst nuclear accident since the 1986 Chernobyl incidence. The multiple meltdowns and release of radiation mandated an enforced exclusion zone around the Fukushima Dai-ichi NPP, which remained off limits for the remainder of 2011 due to the area's elevated radiation levels.

Extensive post tsunami surveys were conducted under the coordination of the Joint Survey Group (TTSG), which was established on the day after the event. Based on established protocols tsunami surveys should be performed as quickly as possible without interfering with initial rescue operations, but prior to perishable evidence being removed during recovery and reconstruction. Given the scale of this event with an affected area spanning more than 1,000 km, a comprehensive survey was facilitated

through collaborative efforts by numerous teams involving various organizations, disciplines and countries. About 300 Japanese and international researchers from multiple disciplines participated in the Joint Tsunami Survey Group (Mori et al., 2012). Rapid sharing of collected data enabled coordination among individual survey teams to complement and fill data gaps, while limiting redundant surveys. The evolving database updated on the Internet provided continuous public access for scientific research as well as rescue, recovery and restoration efforts in the affected areas.

Here we report the findings from the first comprehensive tsunami survey in the southern portion of Minami-Soma, Fukushima Prefecture. Our field survey in this area had been delayed by the exclusion zone imposed after the multiple meltdowns and release of radiation at the Fukushima Dai-ichi NPP. We focus on the spatial distribution of tsunami inundation heights as well as damage to protective coastal structures such as seawalls. Since the nuclear accident was primarily caused by tsunami inundation, it is important to understand the detailed tsunami effects along this stretch of coastline. The Fukushima coast is distinguished by different topographic and bathymetric features from the Sanriku and Sendai coasts further north. Almost all human beings, except a few workers at the nuclear power plants, were displaced from the area. Fortunately many tsunami watermarks were preserved for over a year given the complete lack of human activities including postponed clean-up, recovery and reconstruction efforts.

2. Coastal topography and tsunami inundation in Minami-Soma

The coastal topography and tsunami watermark heights to the north of the Fukushima Dai-ichi NPP up to the Sendai Plain are shown in Figure 1. The measured tsunami heights obtained by Sato et al. (2013) and those compiled by the Joint Survey

Group to the north of the original 20 km exclusion zone are also included in Figure 1 and compared with nearshore tsunami heights at the water depth of 10 m computed by Sato et al. (2013).

The shoreline of the Fukushima Prefecture is straight with a slightly convex curvature in contrast to the concave and low lying bight along the Sendai Plain further north. The coastline in Minami-Soma is characterized by a repetitious pattern of coastal bluff formations (typically 20 m high) and small coastal plains (less than 2 km wide). Coastal cliffs reach heights up to 40 m above sea level along the central Fukushima Coast. Small rivers separate these hills and form confined low-lying coastal plains. The overall distribution of tsunami heights is influenced by the coastal topography (Figure 1). The tsunami height is relatively low along the Sendai Plain, reflecting the divergence of wave rays by refraction associated with the concave bathymetry in combination with the wide continental shelf. The low lying Sendai Plain allowed the tsunami inundation to penetrate several kilometers inland, while gradually attenuating its energy and height. In comparison, the tsunami heights along the Fukushima Coast increased due to the convex shaped shoreline and the associated offshore bathymetry, which tend to focus tsunami energy (Sato et al., 2013).

Prior to the 2011 event, the coastal plains were protected by seawalls with a design height of 6 m T.P. Tokyo Peil (T.P.) is the standard topographic datum in Japan and representing the mean sea level in Tokyo Bay. Many seawalls collapsed due to the hydrodynamic loading from tsunamis with their onshore heights of 10 to 15 m, thereby far exceeding the seawall design height of 6 m. Co-seismic land-level subsidence of 0.5 m in the area further reduced the effective seawall height. Figure 2 shows large flooded areas one day after the tsunami attack. Inundated flat coastal plains with standing water

affected by the land subsidence are separated by a series of coastal bluffs aligned to the shoreline. The following inundation areas are the focus of our investigation: from north to south, ‘Obama’ denotes the coastal plain around the Ohtagawa River, ‘Tsukabara’ denotes the coastal plain around the Odaka River, ‘Murakami’ denotes the isolated circular hill on the coast, ‘Tsunobeuchi’ denotes a relatively narrow coastal plain south of Murakami, and ‘Idagawa’ denotes a coastal plain around the Miyata River.[#]

As noted earlier in Section 1, post-tsunami surveys in the southern portion of Minami-Soma were delayed owing to the nuclear accident, which isolated coastal areas within the exclusion zone. All human activities were restricted within 20 km radius from the Fukushima Dai-ichi NPP after the infamous hydrogen explosions (the first one occurred on March 12, one day after the tsunami attack), and the residents were completely evacuated by the 5th day (March 16). Entry into the area was prohibited and access strictly controlled. In February 2012, less than one year after the tsunami event, the survey team organized by the University of Tokyo and Fukushima Prefecture was granted a special permit and conducted the first tsunami survey along the coast of the entire exclusion zone (Sato et al., 2013). In this paper we report the findings of a follow-up survey performed on June 19-20, 2012 as the access restriction was lifted for the coastal areas in the southern Minami-Soma. To our knowledge, this represents the only detailed tsunami survey conducted in the previously restricted areas of Minami-Soma.

As shown in Figure 3, many clear tsunami watermarks, such as mudlines representing the inundation levels on buildings, were found intact even more than one

[#]Obama (37°35.5’N 141°01.5’E); Tsukabara (37°34.5’N 141°01.5’E); Murakami (37°33.1’N 141°01.6’E); Tsunobeuchi (37°32.6’N 141°01.7’E); Idagawa (37°31.8’N 141°01.8’E).

year after the tsunami inundation. We could easily identify and record tsunami borne debris stranded in sheltered locations such as inside houses, tsunami-induced damage marks on communication towers, and breakage of tree limbs. (Note that all watermark photographs are archived and available on the Internet in Tsunami Joint Survey Group Photo Archive, 2013). This highlights that some tsunami watermarks can remain preserved for an extended time under the absence of human activities such as clean-up, recovery and reconstruction.

Hydrodynamic tsunami modeling suggests focusing of tsunami wave energy towards Minami-Soma (Sato et al., 2013). The computation was based on the linear long-wave theory with the use of the tsunami source estimated by Fujii et al. (2011). Figure 4 illustrates distribution of maximum water level due to tsunami. The numerical simulation suggests that the refraction of tsunami due to bathymetry played an important role in the propagation direction and the local tsunami amplification. Note that one of the local peaks appears to be headed towards Minami-Soma.

Based on videos and photos recorded by local residents, the tsunami reached the shore in the form of a breaking bore with a height of about 10 m (Sato et al., 2013, Sanuki et al., 2013). When the bore impacted coastal cliffs or seawalls, the deflected water splashed up to heights of 20 to 30 m. The formation of such high splash-up near the shoreline is confirmed in a series of photographs recorded at Tsukabara (Figure 5). Examining the successive series of photographs with the time interval of 0.5 s (only three snapshots are shown in Figure 5a, b and c), the incident tsunami direction is inferred from the location of the two surviving pine trees (about 20 m high above sea level based on laser field measurements) marked by arrows in subsequent images in Figure 5. The tsunami initially attacked the area from the southeast (15:39:24, according

to the camera time stamp) and seconds later also from the northeast (15:39:28 and 15:39:34).

Shimozono et al. (2012) numerically simulated tsunami inundation processes for many localities affected by the 2011 Tohoku Tsunami and compared the results with field measurements, discussing the effect of topographic slope on inland inundation heights. The topographic slope affects the energy dissipation in the tsunami runup process. The longer the tsunami penetration distance on mild slope is, the greater the resulting energy loss. This trend is confirmed by the sharp contrast in inland tsunami behavior observed between the Sanriku and Sendai Coasts. The steep slope topography along the Sanriku Coast resulted in high tsunami runup near the maximum tsunami penetration, while the mild slope topography in the Sendai Plain exhibits tsunami heights decaying with distance from the shore. In the Sendai Plain the runup heights at the inundation limit are significantly lower than corresponding tsunami heights near the shore. Funneling inland topography commonly found on the steep ria-type Sanriku coast further enhanced the amplification of tsunami runup (e.g., Shimozono et al., 2014). Similar variation in onshore tsunami behavior was found along the Fukushima Coast.

Figure 6 shows tsunami heights measured at Kabaniwa, Soma (see Figure 1 for the location)[†]. The inland topography of Kabaniwa is a V-shaped valley. The coastline was protected by a concrete rip-rap type mound seawall topped by a curved capping wall with the total height of 6 m T.P. The tsunami completely destroyed the seawalls to the ground level as shown in Figure 7 (a). The maximum runup location is shown in Figure 7 (b), where the tsunami height increased with the distance from the shore to the runup

[†] Tsunami watermarks were measured by the RTK-GPS system with Virtual Reference Station mode with positional accuracy of a few centimeters.

height at about 500 m inland (see Figure 6).

The distribution of tsunami heights in Minami-Soma is shown in Figure 8. Large variation in the measured heights is attributed to the coastal features in Minami-Soma characterized by alternating coastal cliffs and plains. The large variation in tsunami height can be described as follows: tsunami heights near geomorphological transitions between the coastal plain and the bluff are much higher than the heights measured within the plain. This is due to tsunami reflection on the bluff, resulting in wave amplification causing the converging flow from the amplified water level in front of the bluff to rush into the coastal plain. This is confirmed in Figures 9 and 10. Figure 9 shows the relationship between the tsunami height and the local ground elevation, whereas Figure 10 shows the relationship between the tsunami height and the distance from the shoreline. Large tsunami heights in excess of 10 m are generally observed at high ground elevations on the slopes of coastal bluffs with exception of a few points at Idagawa marked in Figure 9. Large tsunami heights were observed within 500 m from the shoreline (Figure 10). However inland tsunami inundation heights at different locations vary in spite of comparable tsunami heights near the shore. The tsunami heights more than 1.5 km inland at Obama are as high as 7 m, while those at Idagawa are smaller than 3 m. The reason for this significant difference remains unclear, but could be associated with the difference in damage levels to coastal structures (seawalls) as discussed later in Section 3.

Figure 11 shows aerial photos of Idagawa indicating the locations of the four measurements marked in Figure 9. The photo taken before the tsunami (Figure 11a) shows that the measurement points are located near or inside the coastal pine tree forest, which was approximately 100 m wide and used to exist behind the seawall. Most of the

trees were completely washed away by the tsunami. Only 6 trees survived, which provided tsunami watermarks such as broken branches along with scratch marks on the bark of tree trunks. It is noted that devastating destruction of so called “tsunami control forests” by the tsunami was also observed at Rikuzentakata, Iwate Prefecture (Liu et al, 2013).

Broken tree branches, as well as the damage marks on the two nearby communication towers, at Idagawa indicate that the tsunami reached 11 to 13 m above ground at terrain elevation of about 1.5 m above sea level. Such large tsunami heights are attributed to the flow deflection by seawalls and the initially increased flow resistance induced by the dense coastal pine forest. Similarly at Futaba Beach, located 6 km south of Idagawa and 4 km north of the Fukushima Dai-ichi NPP, a 16.9 m high watermark was measured in the forest while nearby watermarks adjacent to the forest were 12.2 m and 13.6 m (Sato et al., 2013).

3. Damage to coastal structures

Many seawalls were damaged along the Fukushima Coast, which hosts both the Fukushima Dai-ichi and Dai-ni nuclear power plants. Understanding the destruction mechanism of coastal structures in Fukushima is important since the heights of the tsunami exceeded those of the structures by several meters. Studying seawall overtopping flows is crucial to understand the vulnerability of structures as documented by Sato et al. (2012) in a field study at Nakoso located at the southern end of the Fukushima Prefecture.

Kato et al. (2012) compiled a comprehensive dataset of seawall destruction due to the 2011 Tohoku Tsunami. On the basis of visual inspection of aerial photographs and

satellite images, they categorized the destruction of seawalls in ‘complete collapse’ when the seawall completely collapsed to the ground level, and ‘partial collapse’ when some part of seawall remained. Table 1 summarizes the data for seawalls in Minami-Soma (locations are identified in Figure 2). The ratio of ‘complete collapse’ is large at Obama, which may explain why the tsunami heights near the inundation limit at Obama were large compared to Idagawa (Figure 9). This suggests that unless the protective coastal structures (seawalls) were completely destroyed, the remnant seawalls are capable of reducing the inland inundation level.

Based on the lessons learned from the Tohoku Tsunami, the Japanese Government introduced two-level tsunami hazards to deal with tsunami disaster mitigation. The first-level tsunami hazard (Level-1 tsunami) is defined as a frequent tsunami with the return period of one hundred years. Shore protection structures are designed for a Level-1 tsunami, which dictates crown elevations along with other design criteria. On the other hand, the second-level tsunami hazard (Level-2 tsunami) represents the probable maximum tsunami and is used to establish evacuation strategies and plans. The return period of the Level-2 tsunami is set at one thousand years. Partially damaged protective coastal structures (e.g. seawalls) remain capable of reducing tsunami effects for tsunamis exceeding their design level (Level-1). Hence the structures should remain partially effective for a Level-2 event, unless the structures were totally destroyed. Therefore, it is important to construct such protective structures with the consideration of tsunamis beyond the design level (Level-1). In other words, protective coastal structures like tsunami seawalls should be designed to maintain partial effectiveness even for “beyond-the-design-basis” conditions. This design concept is called “nebari” in Japanese, which implies tenacity, toughness and resilience. Careful field observations

on damaged seawalls should lead to some insights for how to design seawalls using the ‘nebari’ concept. However this concept should not be applied to critical infrastructure such as nuclear power plants where overtopping must be prevented.

Figure 12 shows a partially damaged seawall at Isobe in Soma City (see Figure 1 for location). The gently sloped front face is intact but significant damage was found on the crown and along the landward slope. A large amount of water impounded on the lee side of the seawall filled a scour hole excavated by the extensive tsunami overtopping flow. The detached rubble mound breakwaters located about 100 m offshore of the seawall appeared to be intact.

The Tsukabara coast was also protected by seawalls with a crest height of 6 m T.P. Figure 13 shows upright concrete seawalls completely broken off at the ground level. The 3 m wide capping concrete plate and the landside concrete plate were displaced and transported inland by the overflowing tsunami. The sand filled core inside the seawall was completely washed away. The progressive collapse and scour removed the backside support leading to the fracture at ground level of the seaside concrete wall. Some of the concrete armor blocks, originally placed in front of the seawall, were found more than 300 m inland.

Figure 14 shows a surviving seawall on the south side of the Odaka River in Tsukabara. The gentle slope of the front face and the crown of the seawall are intact. The landward side is partly collapsed, but the gravel land fill which had been placed to cover the landward slope of the seawall appeared to minimize the scour there.

The foregoing observations on seawall failures suggest that design improvements for the crown portion and the lee side of the seawalls are important to enhance “nebari” under overtopping flow. For example, a heavier crown cap combined with milder side

slopes could help reduce damage to the seawall. Furthermore, a concrete apron extended landward from the lee-side toe of the sea wall could reduce scour actions. Another example of a remnant seawall is shown in Figure 15, indicating that the presence of partitioning walls was effective in supporting the seawall even where a substantial amount of the fill material was scoured away. Black sand bags were placed in the section of total failure, where partitioning walls were not installed (Figure 15). The foregoing and many other observations should be analyzed carefully to develop the designs of future protective coastal structures based on “nebari.”

Figure 16 shows the destruction of the Odaka Pump House located close to the shoreline along the Idagawa Coast (see Figure 11 for the location). The pump house is a reinforced-concrete structure which failed completely as indicated by fractured walls and columns snapped off at their base. Observed scour holes around the foundation of the pump house did not appear to contribute to the structural failure. The seawalls initially blocked the incident tsunami flow allowing energy storage and accumulation until overtopping commenced. This stored energy – *at least* to the crown elevation (6.1 m) of the seawall – must have been released to the lee side. The overtopping flow released from the high elevation of the seawall crown created a high-velocity (more than 11 m/s based on the Bernoulli theorem) onto the initially dry soil surface behind the seawall. The upper limit of the flow speed is estimated to 17 m/s for a tsunami height of 15 m near the seawall at Idagawa (Figure 9). Therefore, the flow speed behind the seawall in Idagawa is constrained within a range of 11 ~ 17 m/s, which is comparable to velocity measurements at Kesenuma (Fritz et al., 2012). The corresponding stagnant pressure range is 61 ~ 145 kPa, which could explain the massive fluid forces applied to any trees and structures behind the seawall. The generation of

such massive hydrodynamic forces by overtopping flows immediately behind the seawall can be considered as one of the disadvantages of seawalls. Protective coastal structures limit the ocean view and the noise from an approaching tsunami, which in combination with psychological overconfidence in engineered defense structures, could mislead people to delay their evacuation. In Japan, signs on coastal structures remind residents to heed evacuations regardless of the engineered defenses.

4. Conclusions

This paper described the results of the detailed tsunami survey in Minami-Soma, where the survey was delayed due to the nuclear accident at the Fukushima Dai-ichi Nuclear Power Plant. The main findings are summarized as follows:

- (1) Tsunami inundation heights in Fukushima Prefecture were relatively large owing to the macroscopic features in offshore bathymetry and the convex shape of the coastline. The variation in tsunami inundation height was significant in Minami-Soma reflecting alternating coastal bluffs and plains. Large tsunami heights exceeding 10 m were found within 500 m from the shoreline. Tsunami reflection by seawalls and cliffs, and increased flow resistance induced by coastal pine forest belts are considered to be the cause of local and temporal amplifications in areas near the shore.
- (2) Distribution of the inland tsunami height profile was dependent on the inland topography. Steep V-shaped valleys produced landward increasing tsunami heights, while across flat coastal plains tsunami heights decayed with distance from the shoreline.
- (3) Protective coastal structures (e.g. seawalls) as well as dense coastal forests

temporarily slow down the incident tsunami, while absorbing and accumulating tsunami potential energy. The sudden release of the stored tsunami energy as the forests collapsed and walls were overtopped resulted in significant hydrodynamic forces along with debris impact and associated damming forces causing unanticipated structural damage and scour in the areas immediately behind the seawalls or coastal forests.

- (4) Unless completely destroyed, seawalls were effective in reducing tsunami inundation levels. Some remnant seawalls provided valuable design lessons in enhancing the tenacity of seawalls against tsunami overflow. Gentle side slopes, landfill on the landward slope and placement of partitioning walls are considered among enhancement factors to strengthen seawalls by using the concept of ‘nebari’, a Japanese word representing tenacity, toughness and resilience.

5. Acknowledgments

The authors of UT and TUMST were supported by Japan Science and Technology Agency through the J-RAPID program. H.Y. and H.M.F. were supported by the US National Science Foundation through the NSF RAPID award CMMI-1135768. The authors also acknowledge field survey assistance by several students of UT and TUMST.

6. References

Fritz, H.M., Phillips, D.A., Okayasu, A., Shimozone, T., Liu, H., Mohammed, F., Skanavis, V., Synolakis, C.E., Takahashi, T. (2012). 2011 Japan tsunami current velocity measurements from survivor videos at Kesennuma Bay using LiDAR,

- Geophys. Res. Lett.*, 39, L00G23, doi:10.1029/2011GL050686.
- Fujii, Y., K. Satake, S. Sakai, M. Shinohara and T. Kanazawa : Tsunami source of the 2011 off the Pacific coast of Tohoku Earthquake, *Earth Planets Space*, Vol. 63 (No. 7), pp. 815-820, 2011.
- Kato, F., Y. Suwa, K. Watanabe and S. Hatogai: Damages to shore protection facilities induced by the Great East Japan Earthquake Tsunami, *Journal of Disaster Research*, Vol.8 No.4, 612-625, 2013.
- Liu, H., Shimosono, T., Takagawa, T., Okayasu, A., Fritz, H.M., Sato, S., Tajima, Y.: The 11 March 2011 Tohoku Tsunami survey in Rikuzentakata and comparison with historical events. *Pure Appl. Geophys.*, 170(6-8):1033-1046, doi:10.1007/s00024-012-0496-2, 2013.
- Mori, N., Takahashi, T. and The 2011 Tohoku Earthquake Tsunami Joint Survey Group : Nationwide post event survey and analysis of the 2011 Tohoku Earthquake Tsunami, *Coastal Engineering Journal*, JSCE, 54(1), 1250001, 2012.
- Sanuki, H., Y. Tajima, H. Yeh and S. Sato : Dynamics of tsunami flooding to river basin, *Proc. Coastal Dynamics*, 2013.
- Sato, S., S. Takewaka, H. Liu and H. Nobuoka : Tsunami damages of Nakoso Coast due to the 2011 Tohoku Tsunami, *Proc. 33rd Intl. Conf. on Coastal Engineering*, 2012.
- Sato, S., H. Yeh, M. Isobe, K. Mizuhashi, H. Aizawa and H. Ashino : Coastal and nearshore behaviors of the 2011 Tohoku Tsunami along the central Fukushima Coast, *Proc. Coastal Dynamics*, 2013.
- Sato, S.: 2011 Tohoku Tsunami and future directions for tsunami disaster mitigation, *Keynote lecture, Proc. of 2013 IAHR Congress*, Tsinghua University Press, 2013.
- Shimosono, T., S. Sato, A. Okayasu, Y. Tajima, H. M. Fritz, H. Liu and T. Takagawa:

- Propagation and inundation characteristics of the 2011 Tohoku Tsunami on the central Sanriku Coast, *Coastal Engineering Journal*, JSCE, 54(1), 1250004, 2012.
- Shimozono, T., H. Cui, J. D. Pietrzak, H. M. Fritz, A. Okayasu and A. J. Hooper: Short wave amplification and extreme runup by the 2011 Tohoku Tsunami, *Pure Appl. Geophys.*, 2014 (submitted).
- Simons, M., S.E. Minson, A. Sladen, F. Ortega, J. Jiang, S.E. Owen, L. Meng, J.-P. Ampuero, S. Wei, R. Chu, D.V. Helmberger, H. Kanamori, E. Hetland, A.W. Moore, and F.H. Webb: The 2011 Magnitude 9.0 Tohoku-Oki Earthquake: Mosaicking the Megathrust from Seconds to Centuries. *Science*, 332:1421-1425. doi:10.1126/science.1206731, 2011.
- Tohoku Tsunami Joint Survey Group (TTSG): Tsunami survey database, <http://www.coastal.jp/tsunami2011/>, referred on October 2013.
- Tsunami Joint Survey Group Photo Archive: <http://grene-city.csis.u-tokyo.ac.jp/>, referred on October 2013.

LIST OF FIGURES & TABLES

Figure 1 Distributions of measured tsunami heights around the study area. The thin solid line represents the nearshore tsunami height at the water depth of 10 m computed by Sato et al. (2013).

Figure 2 Aerial photo of Minami-Soma, March 12, 2011, courtesy Dr. K. Satake, UT.

Figure 3 A clear mudline watermark around the exterior of a residential house located 1.2 km from the shoreline at Idagawa, Minami-Soma (tagged with RPDJ-0017 in TTSG database, June 19, 2012. Note that all watermark photographs are archived and available on the Photo Archives with URL listed in the references).

Figure 4 Maximum water level due to computed tsunami (Sato et al., 2013).

Figure 5 (a)-(d) Tsunami observed at Tsukabara, Minami-Soma (Photographs courtesy Mr. Sadatsugu Tomisawa).

Figure 6 Distribution of measured tsunami heights in Kabaniwa, Soma.

Figure 7 Photos of Kabaniwa, Soma, displaying (a) completely broken seawall and (b) location near the maximum runup (June 20, 2012).

Figure 8 Distributions of measured tsunami heights in the study area.

Figure 9 Relationship between tsunami heights and ground elevations.

Figure 10 Relationship between tsunami heights and distance from the shoreline.

Figure 11 (a), (b) Aerial photos before and after tsunami showing a band of coastal pine trees (Photos are taken by Geospatial Information Authority Japan). Note that the forest remained unchanged in a satellite image taken in November 2009.

Table 1 Total and collapsed length of seawalls in Minami-Soma compiled by Kato et al. (2013).

Figure 12 Seawall damage observed in Isobe, Soma (June 20, 2012).

Figure 13 Seawall damage observed in Tsukabara, Minami-Soma (September 3, 2012).

Figure 14 A surviving seawall observed in Tsukabara, Minami-Soma (June 20, 2012).

Figure 15 A surviving seawall connected with a completely broken section observed in Naraha (August 24, 2012) approximately 20 km south of the Fukushima Dai-ichi Power Plant.

Figure 16 Devastating damage of the Odaka Pump House located close to the Idagawa Coast (February 6, 2012).

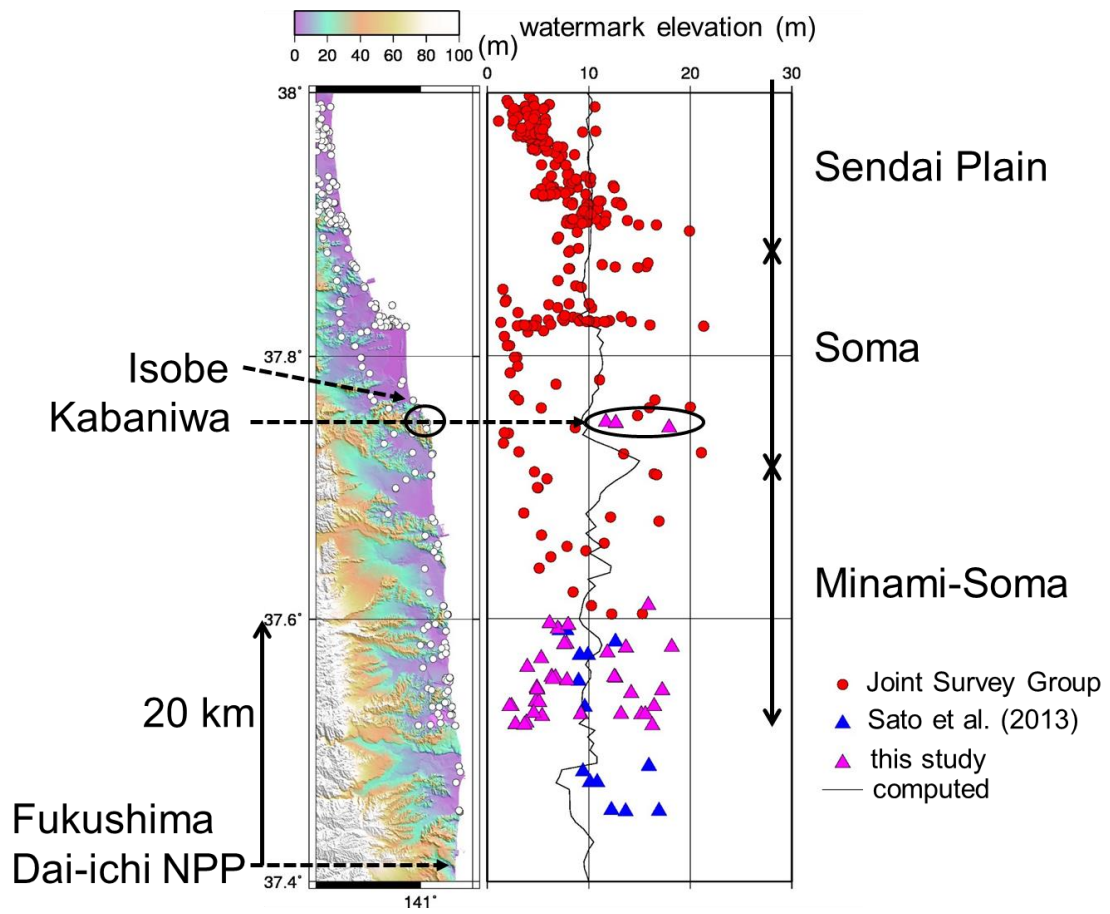


Figure 1 Distributions of measured tsunami heights around the study area. The thin solid line represents the nearshore tsunami height at the water depth of 10 m computed by Sato et al. (2013).



Figure 2 Aerial photo of Minami-Soma, March 12, 2011, courtesy Dr. K. Satake, UT.



Figure 3 A clear mudline watermark around the exterior of a residential house located 1.2 km from the shoreline at Idagawa, Minami-Soma (tagged with RPDJ-0017 in TTSG database, June 19, 2012. Note that all watermark photographs are archived and available on the Internet with URL listed in the references).

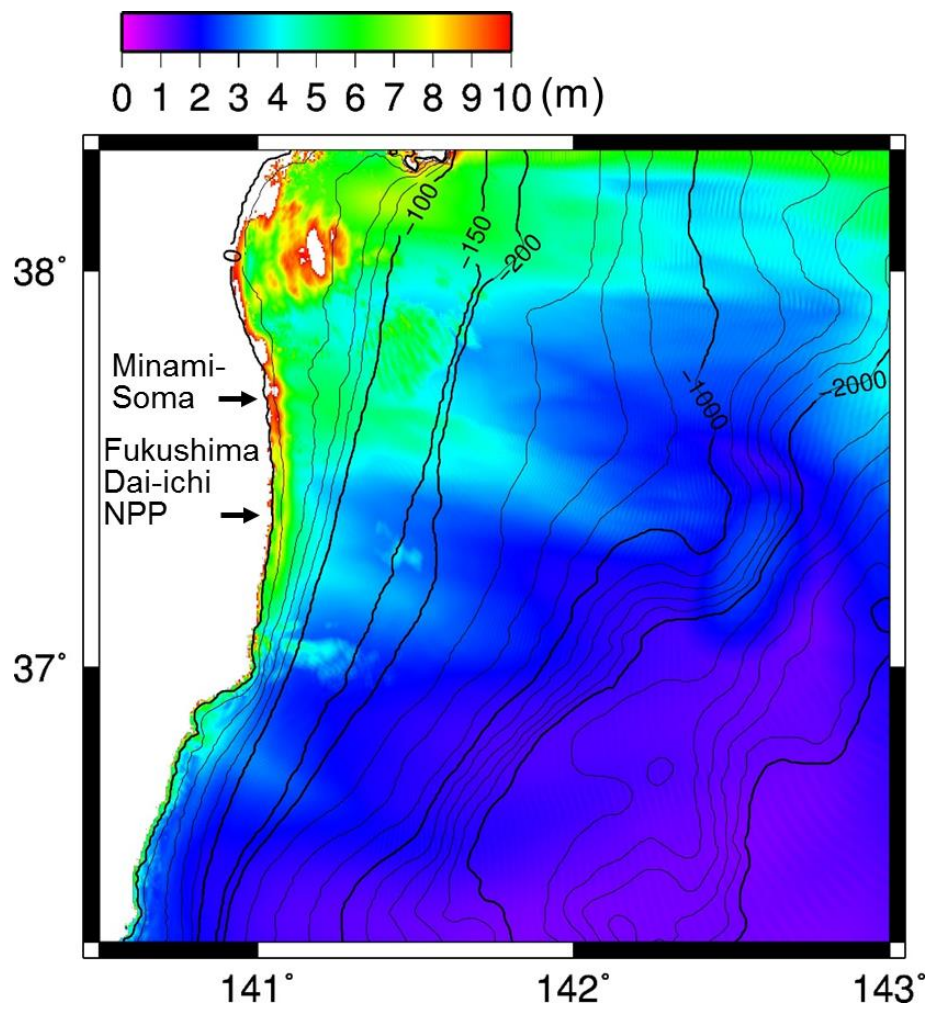


Figure 4 Maximum water level due to computed tsunami (Sato et al., 2013).



Figure 5 (a)-(d) Tsunami observed at Tsukabara, Minami-Soma (Photographs courtesy Mr. Sadatsugu Tomisawa).

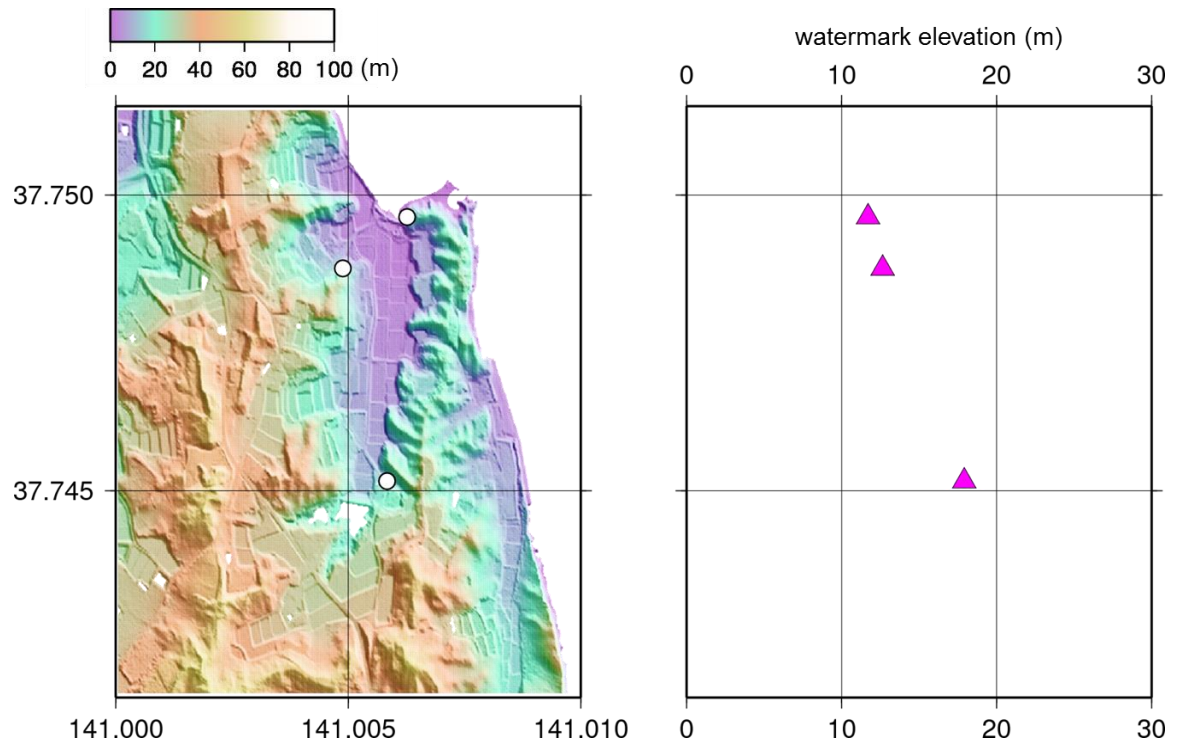


Figure 6 Distributions of tsunami height in Kabaniwa, Soma.



Figure 7 Photos of Kabaniwa, Soma, displaying (a) completely broken seawall and (b) location near the maximum runup (June 20, 2012).

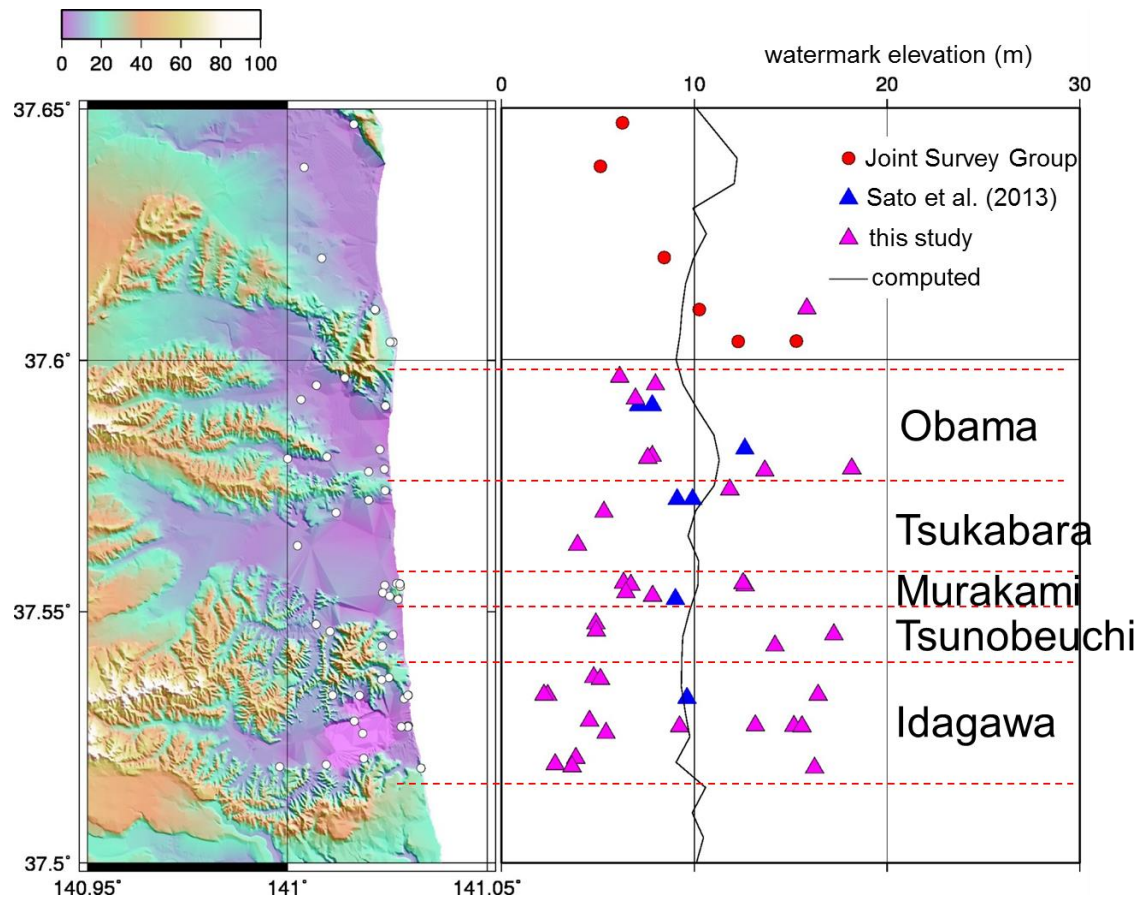


Figure 8 Distributions of measured tsunami heights in the study area.

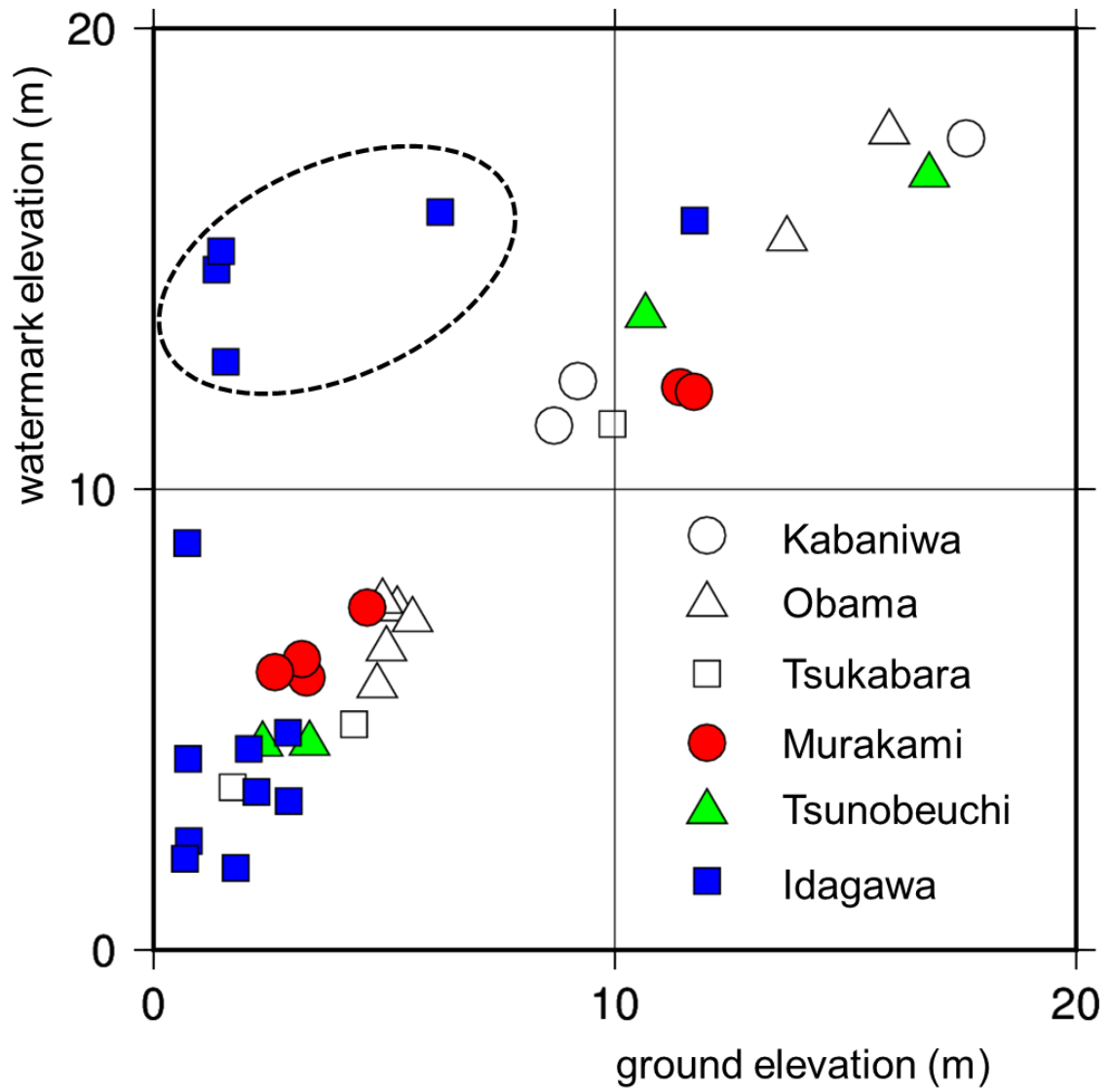


Figure 9 Relationship between tsunami heights and ground elevations.

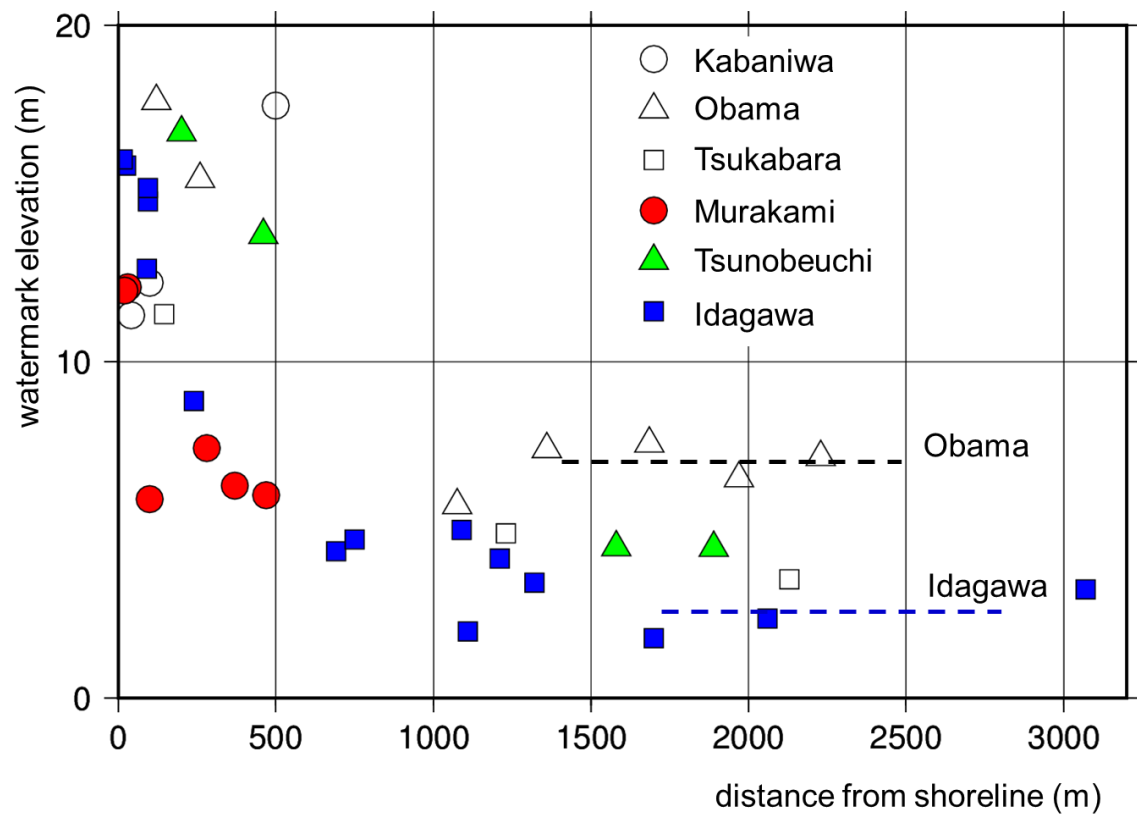
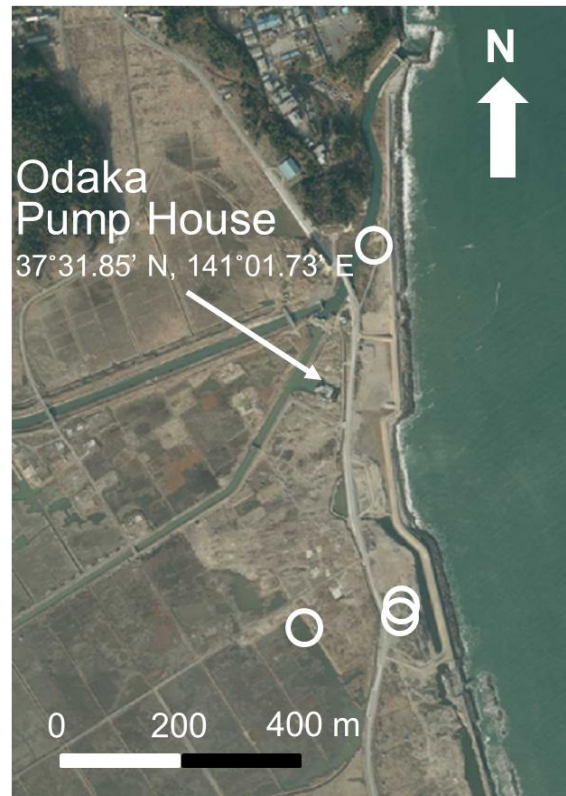


Figure 10 Relationship between tsunami heights and distance from the shoreline.



(a) before tsunami, November 1975



(b) after tsunami, December 2012

Figure 11 (a), (b) Aerial photos before and after tsunami showing a band of coastal pine trees (Photos are taken by Geospatial Information Authority Japan). Note that the forest remained unchanged in a satellite image taken in November 2009.

Area	Total length (m)	Length (m) for 'complete collapse'	Ratio (%)
Obama	1,483	469	32 %
Tsukabara	2,041	99	5 %
Murakami	201	0	0 %
Tsunobeuchi	1,581	61	4 %
Idagawa	1,652	0	0 %

Table 1 Total and collapsed length of seawalls in Minami-Soma compiled by Kato et al. (2013).



Figure 12 Seawall damage observed in Isobe, Soma (June 20, 2012).



Figure 13 Seawall damage observed in Tsukabara, Minami-Soma (September 3, 2012).



Figure 14 A surviving seawall observed in Tsukabara, Minami-Soma (June 20, 2012).



Figure 15 A surviving seawall connected with a completely broken section observed in Naraha (August 24, 2012) approximately 20 km south of the Fukushima Dai-ichi Power Plant.



Figure 16 Devastating damage of the Odaka Pump House located close to the Idagawa Coast (February 6, 2012).